Desalination and Water Treatment
www.deswater.com

doi: 10.5004/dwt.2017.20362

67 (2017) 239–246
March

Selectivity and extraction efficiency studies of 4-nitrophenol adsorption on polyethersulfones/Ag nanocomposite

Ekram Y. Danish[a,*], Hadi M. Marwani[a,b,*], Marya A. Alhazmi[a]

[a]*Department of Chemistry, Faculty of Science, King Abdulaziz University, P.O. Box 80203, Jeddah 21589, Saudi Arabia, Tel. +966-12-6952293; Fax: +966-12-6952292; emails: eydanish@kau.edu.sa (E.Y. Danish), hmarwani@kau.edu.sa (H.M. Marwani)*
[b]*Center of Excellence for Advanced Materials Research (CEAMR), King Abdulaziz University, P.O. Box 80203, Jeddah 21589, Saudi Arabia*

Received 22 July 2016; Accepted 15 November 2016

ABSTRACT

In this study, the effectiveness of newly synthesized polyethersulfones/Ag nanocomposites films, as adsorbents, was evaluated for selective separation of 4-nitrophenol from environmental waters. Three polyethersulfones/Ag nanocomposites films were prepared by varying amounts of incorporated Ag nanoparticles. The selectivity of nanocomposites films was investigated toward three mono-substituted phenolic compounds, including 4-nitrophenol, 4-chlorophenol and 4-methoxyphenol. Based on selectivity study results, 4-nitrophenol was the most quantitatively adsorbed on NC3 thin film (20% v/v), indicating that NC3 thin film was the most selective toward 4-nitrophenol among other compounds. In addition, effects of pH value, initial concentration and contact time on the 4-nitrophenol adsorption by NC3 thin film were examined, in order to optimize adsorption process conditions. The experimental adsorption isotherm data were modelled by classical adsorption isotherms which revealed the high agreement of the Langmuir model with adsorption capacity of 105.93 mg g^{-1}. This result demonstrated that the adsorption system was mainly mono-layer on the homogeneous surface of NC3 adsorbent, which supported the validity of Langmuir sorption isotherm model. Data acquired from kinetic models study indicated that the adsorption of 4-nitrphenol onto the NC3 film followed a pseudo-second-order model. Finally, validation of this method has attained reasonable results for the determination of 4-nitrophenol into real water samples.

Keywords: 4-Nitrophenol; SPE; Batch method; UV–Vis; Adsorption capacity; PES/Ag nanocomposite

1. Introduction

Through recent decades there has been a formidable growth in the manufacture of chemical products and their uses. These developments lead to deduct large amount of chemical wastes and contaminants such as organic compounds and heavy metals into water media, which maybe caused due to alteration of chemical, physical and biological properties of water [1]. Phenol and its derivatives are one of the main organic pollutants in wastewater. They are used as raw materials to produce many products such as petrochemicals, pesticides, pharmaceuticals, plastics and steel industries. As a result of their high toxicity even at low concentrations and ability to accumulate in environmental media, the United States Environmental Protection Agency (USEPA) has drawn up a list of phenolic compounds as major pollutants where a minimum amount of them in wastewater should be less than 1 mg L^{-1} [2,3].

Among these compounds, 4-nitrophenol (4-NP) has been attracted more interest due to its production in large amounts worldwide, highly toxic, carcinogenic and inhibitory compared with other mono-nitrophenols, beside to its high stability and solubility in water [4]. However, 4-NP is the most important for intermediate compounds, used in dyes, engineering polymers and specialty products

* Corresponding author.

for military applications, as well as fuel, additionally to pesticides production as main usage of 4-NP [5,6]. Exposure to 4-NP may cause methemoglobin formation, damage to the central nervous system as well as the liver and kidney, skin and eye irritation. Therefore, USEPA has a list of persistent, bio-accumulative and toxic chemicals, which included 4-NP. Thereby, it is necessary to treat effluents from 4-NP before discharging into environmental water [6–8].

So far, there are several treatment techniques have been used for pollutants separation, including cloud point extraction [9], ion exchange [10], liquid–liquid extraction (LLE) [11,12], co-precipitation [13] and solid-phase extraction (SPE) [14,15]. Although LLE is classical technique to extract pollutants in water samples, SPE is the most popular technique nowadays and plays important part in modern analytical science; due to the reducing usage of organic solvents which may be toxic and harmful unlike to LLE. Moreover, SPE offers several of great benefits involving stability, reusability, simplicity, high selectivity and fast separation rate. In addition, heat treatment in each stage of the process is unrequired [15–17]. The most important factor in SPE method is selecting the proper adsorbent to obtain greater efficiency toward the analyte of interest [18]. Nowadays, there is vast scale of popular adsorbents for SPE method which are used to detect and extract target analytes from aqueous media. These adsorbents may be mineral, organic or biological [19]. For instance, activated carbon (AC) [5,20], low-cost natural adsorbents (clay, zeolite, fly ash and sewage sludge) [21,22], C_{18} [23], graphene oxide [24], carbon nanotubes [25] and polymeric materials [4,26]. In recent years, polymeric adsorbents may be an alternative to AC due to their properties of great surface area and the effectiveness to extract and separate many organic pollutants such as phenolic compounds [27,28].

More recently, nanocomposite-based polymer and noble metals are being received more attention in many research areas. This is as a result of the synergism between polymer–metal that led to higher uptake capacities for inorganic and organic compounds removal as well as chemical stability at a vast range of pH [29,30]. Among noble metals, silver nanoparticles are suitable candidates for different applications; where the advantage of high specific surface area, long-term durability and high interfacial activity [31,32]. In the present study, polymer nanocomposites were synthesized from polyethersulfones (PESs) and Ag nanoparticles. Where PES considered as high performance polymeric material besides that it has excellent oxidative, thermal, hydrolytic stability and good mechanical properties [33]. The analytical efficiency and utility of new nanocomposites films as solid phase sorbents were evaluated toward selected toxic phenols. The selectivity of the prepared PES/Ag nanocomposites films toward three mono-substituted phenols, which include 4-NP, 4-chlorophenol (4-CP) and 4-methoxyphenol (4-MP) was studied. Subsequently, different factors such as pH value, initial concentration of 4-NP and shaking time were tested. Finally, the efficiency of the recommended approach to extract 4-NP was examined by applying it to real water samples.

2. Experimental

2.1. Materials and chemicals

PES with molecular weight of 66 amu and density of 1.37 g/cm^3, cetyltrimethylammonium bromide (CTAB), silver nitrate ($AgNO_3$), sodium borohydride ($NaBH_4$), 1-methyl-2-pyrrolidone (NMP), 4-NP, 4-CP and 4-MP were obtained from Sigma-Aldrich (Milwaukee, WI, USA). The reagents used were of analytical purity grade, and doubly distilled de-ionized water was used during experimental studies.

2.2. Synthesis of silver nanoparticles and nanocomposites

Silver nanoparticles were prepared according to previous reports by Azum et al. [34,35]. CTAB solution was added into silver nitrate solution in 1:1 ratio and then added $NaBH_4$ solution into the above mixture as a reducing agent. Nanocomposites films (NC1, NC2 and NC3) were prepared by adding 0.3, 0.5 and 10 mL silver nanoparticles solution individually to PES/NMP solution (50 mL) and stirred for 1 h. The final solutions were casted on glass slides using a mechanical casting rod of thickness 250 μm and then dried. Eventually, the obtained films were soaked in doubly distilled de-ionized water and removed from the glass plate [36,37].

2.3. Instrumentation

The morphology of nanocomposite was observed by field emission scanning electron microscope (FESEM; JEOL, Japan, JSM-7600F). Energy dispersive X-rays spectrometry (EDS) was carried out for the elemental analysis by using Oxford–EDS system. Crystal structure of nanocomposite was analyzed by execution of X-ray diffraction (XRD) using Thermo scientific diffractometer with a Cu Kα radiations (λ = 0.154 nm) source. UV–Vis spectrophotometer (MultiSpec 1501; Shimadzu, Japan) was used for spectrophotometric analysis of phenolic compounds solutions. A pH meter Jenway 3505 (CamLab, UK) was operated to measure pH values with absolute accuracy limits, using National Institute of Standards and Technology buffers.

2.4. Maximum absorbance and calibration curve

The concentrations of phenolic compounds before and after equilibrium were measured spectrophotometrically. Absorbance of analytes was measured at 223 nm for 4-CP and 4-MP. Whereas for 4-NP the wavelength detection was 317 nm for pH ≤ 6 and 400 nm for pH ≥ 7 because of the incidence of redshift on maximum absorbance in basic medium. Standard calibration curves for phenolic compounds were linear (R^2 > 0.9995) in the concentrations range 5–200 mg L^{-1}. The concentrated solutions were diluted to fall within absorbance range of less than 1.0 for ensuring accurate detection of UV–Vis spectrometer sensitively.

2.5. Batch adsorption procedure

Stock solutions of 4-NP, 4-CP and 4-MP were prepared using distilled de-ionized water and kept in cool and dark place. For selectivity investigations, all standard solutions of mono-substituted phenolic compounds (10 mg L^{-1}) were mixed individually with 20 mg of thin film (NC1, NC2 and NC3). Then, the prepared mixtures were shaken in a shaker bath for 1 h and constant temperature of 25°C. Further, the phenolic solutions were separated from thin film by filtration, and the final concentration of 4-NP (or other phenols) was measured

spectrophotometrically. In order to examine the pH effect on 4-NP extraction performance, selected concentration of 4-NP solutions (10 mg L^{-1}) were prepared and adjusted to different values of pH, ranging from 1.0 to 12.0, using appropriate buffer aqueous solutions by adding 0.2 mol L^{-1} HCl/KCl to reach pH 1.0 and 2.0, 0.1 mol L^{-1} CH_3COOH/CH_3COONa for pH 3.0–6.0, and Na_2HPO_4/HCl and Na_2HPO_4/NaOH for pH 7.0–9.0 and 10.0–12.0, respectively. For studying the uptake capacity of 4-NP, desired concentrations of 4-NP (5, 10, 15, 20, 30, 40, 50, 60, 70, 100, 150 and 200 mg L^{-1}) were prepared as above by adjusting the pH to the optimum value of 6.0. In addition, the shaking time effect on 4-NP extraction under the same conditions of batch procedure was studied for predetermined period of time, including 2.5, 5, 10, 20, 30, 40, 50 and 60 min.

3. Results and discussion

3.1. Characterization of NC3

NC3 was morphologically characterized by FESEM (Fig. 1). It is clear from FESEM images that pure PES has smooth surface without any particle while NC3 has silver nanoparticles which exist in dispersed as well as aggregated form in polymer matrix. The EDS spectrum (Fig. 2) showed peaks for both polymer as well as silver nanoparticles. EDS spectrum suggests the formation of nanocomposite. XRD was analyzed in order to evaluate the crystallinity of nanocomposite. The XRD pattern (Fig. 3) shows only broad peak at $2\theta = 23°$ which reveal the amorphous nature of NC3. It also shows a weak peak at 44° which suggest the presence of silver nanoparticles in NC3 [38–44].

3.2. Batch adsorption method for 4-NP removal by NC3 thin film

3.2.1. Selectivity study

The selectivity of adsorbents (NC1, NC2 and NC3) for mono-substituted phenolic compounds was evaluated based on the values of distribution coefficient (K_d) and uptake capacity (q_e) of adsorbents. The distribution coefficient value can be defined by Eq. (1) [45]:

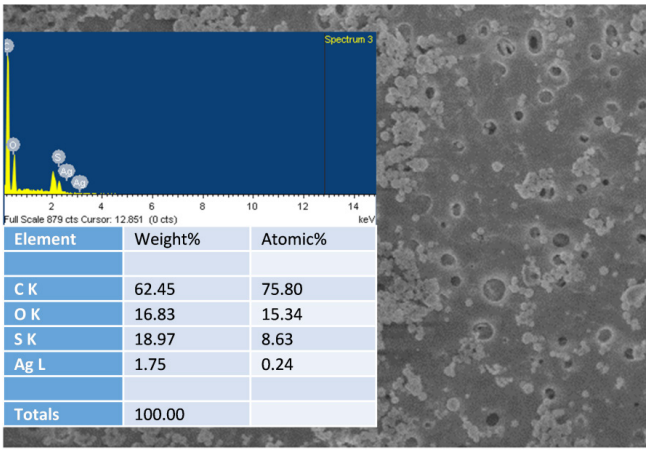

Fig. 2. EDS spectrum of NC3.

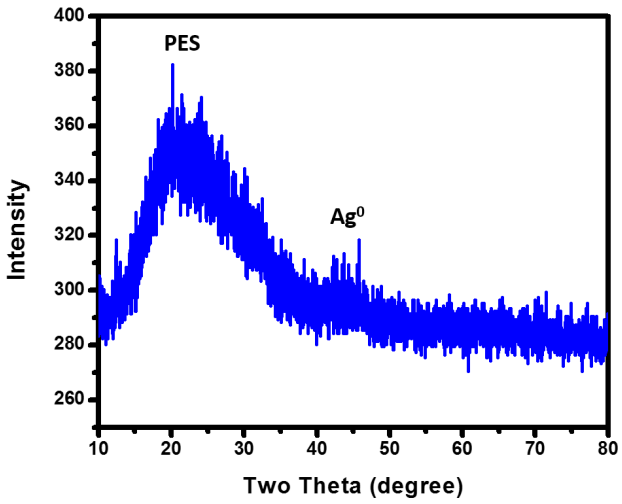

Fig. 3. XRD pattern of NC3.

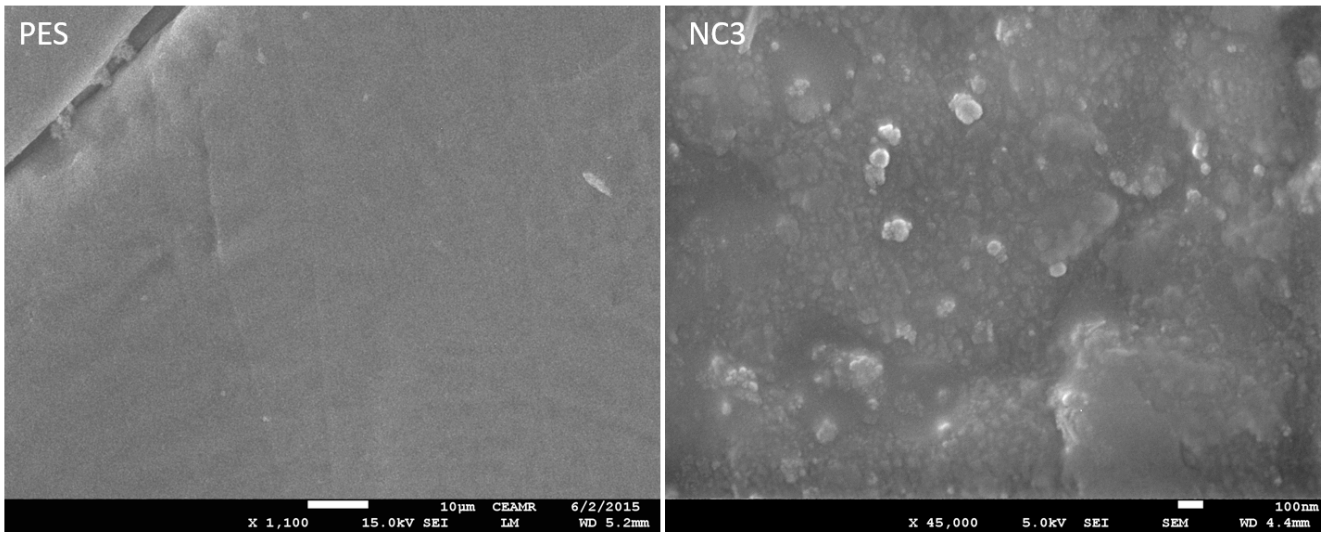

Fig. 1. FESEM images of PES and NC3.

$$K_d = [(C_o - C_e)/C_e] \times [V/m] \quad (1)$$

where C_o indicates the initial concentrations of phenolic compounds (mg L^{-1}) and C_e represents the concentrations after filtration (mg L^{-1}). The V and m parameters correspond to the volume (mL) and solid phase mass (g), respectively. Table 1 illustrates all values of K_d and q_e for compounds included in this study. The results indicated that NC3 thin film was more selective for 4-NP over 4-CP and 4-MP, based on distribution coefficient value.

3.2.2. Influence of pH on adsorption

The effect of pH on 4-NP sorption is very important to study; it plays a significant role on ability of surface charge dissociation for adsorbent as well as adsorbate. Specifically, 4-NP presents in aqueous media as weak organic acid with a pK_a value of 7.2. However, it transforms to its anionic form, 4-nitrophenoxide (4-NP^-), at pH higher than its pK_a. Herein, experiments were performed for 10 mg L^{-1} initial concentration of 4-NP at room temperature with adjusting pH of solutions to several values in the range of 1.0–12.0. Fig. 4 illustrates the pH influence on the extraction percentage of 4-NP. Generally, it can be observed that there is an increase in the 4-NP percentage extraction from 13.43% to 95.10% with increasing pH value from 1.0 to 6.0. Otherwise, pH solutions above 6.0 led to slightly decreasing in 4-NP extraction percentage. This is due to the ionization of 4-NP adsorbate molecules that appears as 4-NP^-. Moreover, the electrostatic repulsions occur between the phenolate–phenolate anions and negative charge of solid surface, led to a redshift in the maximum absorbance (λ_{max}) from 317 to 400 nm when the pH value reaches 7.0 or above (Fig. 5) [46,47]. These results indicated that the adsorption process for 4-NP is strongly dependent on the pH media. Thus, the optimum value of pH solution was selected as pH 6.0 for investigating other factors that may affect the adsorption performance of 4-NP onto NC3 thin film.

Table 1
Selectivity study of (20 mg) different thin films toward different phenolic compounds at 25°C

Phase	Compound	q_e (mg g^{-1})	K_d (mL g^{-1})
NC1 thin film	4-NP	0.97	105.55
NC2 thin film	4-NP	0.63	66.89
NC3 thin film	4-NP	11.50	14,375.00
	4-CP	4.52	708.33
	4-MP	3.19	427.85

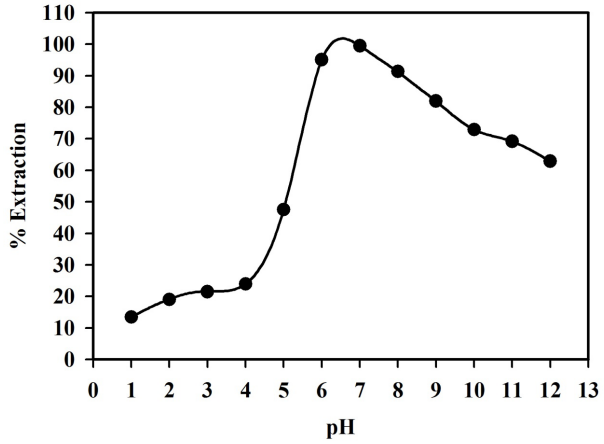

Fig. 4. Effect of pH on the adsorption of 10 mg L^{-1} 4-NP on 20 mg NC3 thin film at 25°C.

3.2.3. Determination of 4-NP uptake capacity

In order to evaluate the effect of 4-NP initial concentration on the uptake capacity of the adsorbent, 20 mg of NC3 thin film was added to 25 mL of 4-NP aqueous solutions with different initial concentrations ranging from 5 to 200 mg L^{-1}, and adjusting these solutions to the optimum pH value (6.0). Then, the mixtures were shaken for 1 h at 25°C, and the adsorbed amount of 4-NP at each level of concentration was determined. The adsorption profile of 4-NP on 20 mg NC3 adsorbent was obtained by plotting the concentration of 4-NP (mg L^{-1}) vs. the adsorbed 4-NP (mg g^{-1}) (Fig. 6). The uptake capacity of NC3 thin film for 4-NP was found to be 103.17 mg g^{-1} (Fig. 6),

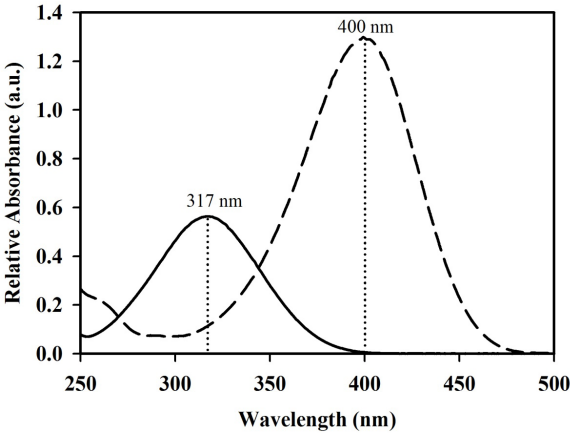

Fig. 5. UV–Vis absorption spectra of 4-NP in acidic medium (solid line) and basic medium (dashed line). Absorbance shift from 317 to 400 nm.

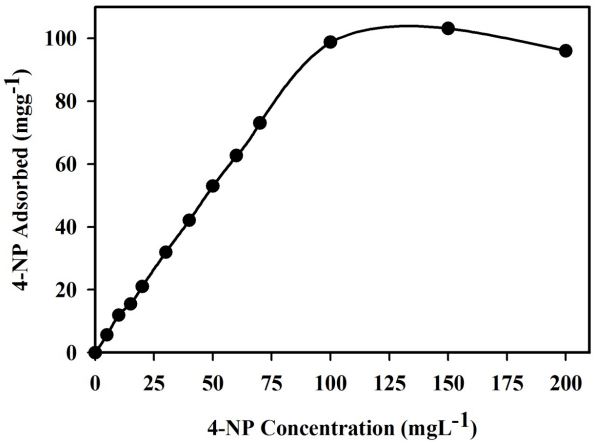

Fig. 6. Adsorption profile of 4-NP on 20 mg NC3 thin film in relation to the concentration at pH 6.0 and 25°C.

which is comparable to other sorbents previously studied for the uptake capacity of 4-NP (181.48 mg g^{-1} [48], 39.38 mg g^{-1} [5], 121.00 mg g^{-1} [49] and 17.28 mg g^{-1} [50]).

3.2.4. Adsorption isotherm models

Adsorption isotherm is an important concept and helpful to describe the nature and mechanism for the adsorption process of adsorbate onto solid adsorbent. Thus, equilibrium isotherm models are utilized for interpreting the experimental data, in which Langmuir and Freundlich are the most used equilibrium models [46,49]. The classical Langmuir model presumes adsorption of a single layer onto homogenous surface of an adsorbent which contains a certain number of sorption active sites. The equation of Langmuir is described as follows:

$$C_e/q_e = (C_e/Q_o) + 1/Q_o b \quad (2)$$

where C_e refers to the equilibrium 4-NP concentration (mg L^{-1}), q_e corresponds to the equilibrium amount adsorbed for 4-NP (mg g^{-1}), Q_o represents the 4-NP adsorption capacity (mg g^{-1}) and the symbol b refers the Langmuir constant (L mg^{-1}) [51].

Fig. 7 shows that plotting C_e/q_e vs. C_e lead to a straight line with a slope of $1/Q_o$ and intercept of $1/Q_o b$. The symbol b can be used for calculating the dimensionless constant separation parameter (R_L), which is able to predict the adsorption system nature if favorable or unfavorable. R_L is obtained from Eq. (3):

$$R_L = 1/(1+bC_o) \quad (3)$$

The adsorption system is considered to be linear if R_L value equals to 1, while favorable sorption if $0 < R_L < 1$ or irreversible if $R_L = 0$ while $R_L > 1$ shows unfavorable process [52].

On the other hand, Freundlich isotherm is proposed a multilayer adsorption onto heterogeneous surfaces, and it can estimated by Eq. (4) [53]:

$$\log q_e = \log K_f + 1/n \log C_e \quad (4)$$

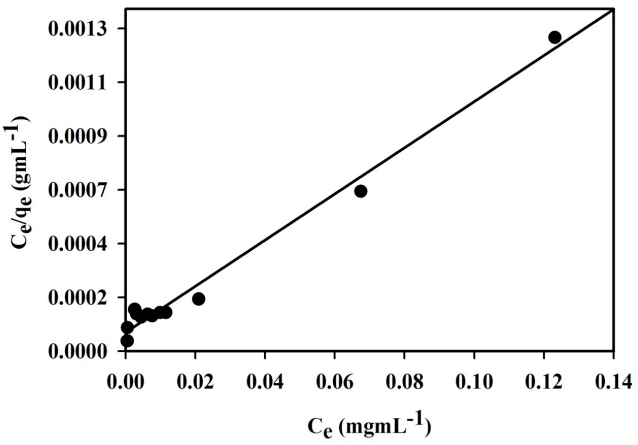

Fig. 7. Langmuir adsorption isotherm model of 4-NP adsorption on 20 mg NC3 thin film at pH 6.0 and 25°C. Adsorption experiments were obtained at different concentrations (5–200 mg L^{-1}) of 4-NP under batch conditions.

where C_e corresponds to 4-NP concentration when adsorption equilibrium is attained (mg L^{-1}) and q_e (mg g^{-1}) refers to the 4-NP adsorbed at equilibrium. The constants of Freundlich recognized as the symbols K_f (mg g^{-1}) and n.

Herein, experimental data of 4-NP adsorption on the NC3 thin film were modelled by above described isotherms. Consequently, it was found that the calculated adsorption capacity value obtained from Langmuir model (105.93 mg g^{-1}) was most closely with that obtained experimentally (103.17 mg g^{-1}), indicating the validity of Langmuir classical model. Thus, the equilibrium isotherm data was suggested the formation of mono-layer of 4-NP adsorbate onto a homogeneous surface of NC3. In addition, R^2 (0.986) and R_L (0.05) values obtained from Langmuir equation confirmed that the adsorption system was favorable based on Langmuir isotherm model.

3.2.5. Effect of extraction time

The effect of contact time is an important factor for batch adsorption method to determine the maximum uptake capacity and study the adsorption kinetics for organic compounds. In order to study the behavior of NC3 thin film adsorption kinetics toward 4-NP, varied shaking times between 2.5 and 60.0 min were chosen. Based on the results, it was observed that the uptake capacity of NC3 thin film for 4-NP speedily increases within 60 min. As displayed in Fig. 8, the adsorbed amount of 4-NP was 92.85 mg g^{-1} after 20 min of the equilibrium period. After 40 min, over 99 mg g^{-1} 4-NP was adsorbed. After 60 min the maximum adsorption of NC3 thin film for 4-NP was found to be 103.17 mg g^{-1}.

3.2.6. Kinetic models

There are several kinetic models which can be used for explaining the mechanisms of adsorption systems. To interpret the data of experimental kinetic, pseudo-first-order and pseudo-second-order sorption kinetic models were utilized in this study. The formula of pseudo-first-order is given by Eq. (5) [54]:

$$\log(q_e - q_t) = \log q_e - (k_1/2.303)t \quad (5)$$

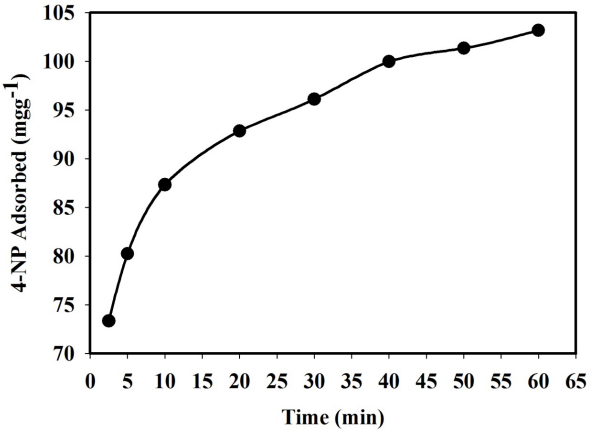

Fig. 8. Effect of contact time on the adsorption of 150 mg L^{-1} 4-NP on 20 mg NC3 thin film at pH 6.0 and 25°C.

where q_t and q_e denote the amounts of 4-NP adsorbed at time t and at equilibrium (mg g^{-1}), respectively, and the symbol k_1 indicates pseudo-first-order rate constant (min^{-1}). Both of sorption rate constant k_1 and uptake capacity q_e for the NC3 thin film were estimated from the intercept and slope of the plot of $\log(q_e - q_t)$ vs. t.

Otherwise, an equation of pseudo-second-order is formulated as Eq. (6) [55]:

$$t/q_t = 1/\upsilon_o + (1/q_e)t \quad (6)$$

where $\upsilon_o = k_2 q_e^2$ (mg g^{-1} min^{-1}) corresponds to the initial sorption rate and k_2 (g mg^{-1} min^{-1}) is the equilibrium rate constant, whereas q_e (mg g^{-1}) and q_t (mg g^{-1}) refer to the amounts of 4-NP on a surface of NC3 phase at equilibrium and at any time t, respectively. Therefore, plotting t/q_t vs. t enables the q_e and υ_o to be found from the intercept and slope, as illustrated in Fig. 9. Accordingly, both of kinetic models have a great correlation coefficient value ($R^2 > 0.99$), and the kinetic factors for these models were listed in Table 2. Data of sorption kinetic were consistent with pseudo-second-order model (Fig. 9). Moreover, the theoretical uptake capacity of 4-NP on NC3 phase calculated from the kinetic equation of pseudo-second-order model (105.16 mg g^{-1}) was well fit with those obtained from the experimental adsorption isotherm (103.17 mg g^{-1}) and Langmuir equation (105.93 mg g^{-1}). Hence, the results supported that nature of kinetic sorption process for 4-NP on NC3 thin film was obeyed the pseudo-second-order model.

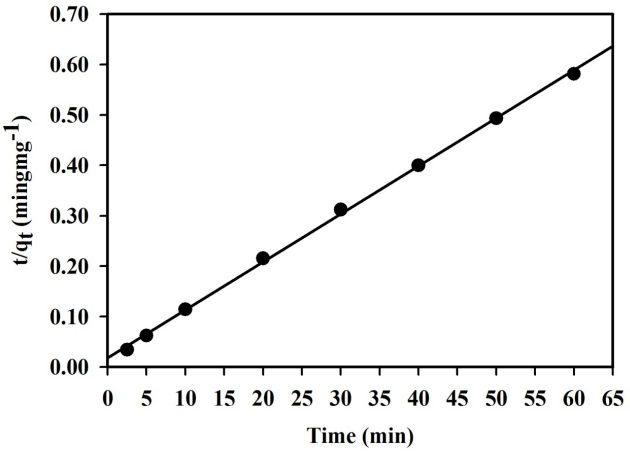

Fig. 9. Pseudo-second-order adsorption kinetic model of 4-NP uptake on 20 mg NC3 thin film at pH 6.0 and 25°C.

Table 2
Calculated parameters of kinetic models for 4-NP adsorption on NC3 thin film at pH 6.0 and 25°C

Kinetic model	R^2	k	q_e (mg g^{-1})
Pseudo-first-order	0.9901	0.0815 min^{-1}	14.60
Pseudo-second-order	0.9991	0.005 g mg^{-1} min^{-1}	105.16

3.2.7. Applicability of the proposed method

In order to ensure the validity of the recommended procedure, the proposed method was applied to the detection and removal of 4-NP from real aqueous samples. The real samples were collected from Jeddah City, Kingdom of Saudi Arabia; including sea water, ground water, lake water, drinking water and wastewater. The standard addition method was carried out by the overall SPE procedure for estimation the accuracy of extraction and removal of 4-NP. The extraction percentage of 4-NP amount in these samples was calculated, and the results were summarized in Table 3. The percentages of 4-NP extracted from the real samples on NC3 thin film were in the range of 88.61%–96.98%. These results indicate the suitability, feasibility and reliability of the proposed method for separating 4-NP from water samples using NC3 thin film.

Table 3
Determination of 4-NP at different concentrations (5, 15 and 25 mg L^{-1}) in real water samples using 20 mg NC3 thin film at pH 6.0 and 25°C ($N = 3$)

Samples	Added (mg L^{-1})	Unadsorbed (mg L^{-1})	Extraction (%)
Ground water	5	0.18 (±0.024)	96.48
	15	0.80 (±0.051)	94.64
	25	1.74 (±0.131)	93.06
Lake water	5	0.21 (±0.038)	95.78
	15	0.82 (±0.055)	94.53
	25	1.86 (±0.157)	92.57
Seawater	5	0.27 (±0.040)	94.65
	15	1.19 (±0.092)	92.06
	25	2.67 (±0.201)	89.31
Drinking water	5	0.15 (±0.019)	96.98
	15	0.71 (±0.048)	95.25
	25	1.68 (±0.125)	93.26
Wastewater	5	0.28 (±0.046)	94.47
	15	1.47 (±0.129)	90.18
	25	2.85 (±0.317)	88.61

4. Conclusions

It can be deduced from the results that PES/Ag nanocomposite film (NC3) is an efficient sorbent for selective separation and detection of 4-NP at trace concentration levels from aqueous solutions. NC3 thin film was also provided high uptake capacity for 4-NP at pH 6.0 and short contact time. Both equations of Langmuir and pseudo-second-order were well fit with experimental results of 4-NP adsorption on NC3 thin film, indicating the fast kinetics of adsorption process by mainly mono-layer of 4-NP onto a homogeneous surface of NC3 thin film. Moreover, the results demonstrate that the proposed method is considered to be agreeable for the selective adsorption and estimation of 4-NP in environmental water samples.

Acknowledgments

This work was supported by the Deanship of Scientific Research (DSR), King Abdulaziz University, Jeddah, under grant No. 363-21-D1437. The authors, therefore, gratefully acknowledge the DSR for technical and financial support.

References

[1] W.S.W. Ngah, S. Fatinathan, Chitosan flakes and chitosan–GLA beads for adsorption of *p*-nitrophenol in aqueous solution, Colloids Surf., A, 277 (2006) 214–222.
[2] M. Abatal, M.T. Olguin, Comparative adsorption behavior between phenol and *p*-nitrophenol by Na- and HDTMA-clinoptilolite-rich tuff, Environ. Earth Sci., 69 (2013) 2691–2698.
[3] Y. Park, G.A. Ayoko, E. Horváth, R. Kurdi, J. Kristof, R.L. Frost, Structural characterisation and environmental application of organoclays for the removal of phenolic compounds, J. Colloid Interface Sci., 393 (2013) 319–334.
[4] E. Marais, T. Nyokong, Adsorption of 4-nitrophenol onto Amberlite IRA-900 modified with metallophthalocyanines, J. Hazard. Mater., 152 (2008) 293–301.
[5] M. Ahmaruzzaman, S. Laxmi Gayatri, Batch adsorption of 4-nitrophenol by acid activated jute stick char: equilibrium, kinetic and thermodynamic studies, Chem. Eng. J., 158 (2010) 173–180.
[6] D. Tang, Z. Zheng, K. Lin, J. Luan, J. Zhang, Adsorption of *p*-nitrophenol from aqueous solutions onto activated carbon fiber, J. Hazard. Mater., 143 (2007) 49–56.
[7] G. Xue, M. Gao, Z. Gu, Z. Luo, Z. Hu, The removal of *p*-nitrophenol from aqueous solutions by adsorption using gemini surfactants modified montmorillonites, Chem. Eng. J., 218 (2013) 223–231.
[8] M. Khatamian, Z. Alaji, Efficient adsorption-photodegradation of 4-nitrophenol in aqueous solution by using ZnO/HZSM-5 nanocomposites, Desalination, 286 (2012) 248–253.
[9] S. Zhong, S.N. Tan, L. Ge, W. Wang, J. Chen, Determination of bisphenol A and naphthols in river water samples by capillary zone electrophoresis after cloud point extraction, Talanta, 85 (2011) 488–492.
[10] M.R. Pourjavid, P. Norouzi, M.R. Ganjali, Light lanthanides determination by fast fourier transform continuous cyclic voltammetry after separation by ion-exchange chromatography, Int. J. Electrochem. Sci., 4 (2009) 923–942.
[11] T. Jiao, C. Li, X. Zhuang, S. Cao, H. Chen, S. Zhang, The new liquid–liquid extraction method for separation of phenolic compounds from coal tar, Chem. Eng. J., 266 (2015) 148–155.
[12] N. Messikh, M.H. Samar, L. Messikh, Neural network analysis of liquid–liquid extraction of phenol from wastewater using TBP solvent, Desalination, 208 (2007) 42–48.
[13] M. Soylak, N.D. Erdogan, Copper(II)–rubeanic acid coprecipitation system for separation–preconcentration of trace metal ions in environmental samples for their flame atomic absorption spectrometric determinations, J. Hazard. Mater., 137 (2006) 1035–1041.
[14] T.-Y. Wang, G.-L. Chen, C.-C. Hsu, S. Vied, E.D. Conte, S.-Y. Suen, Octadecyltrimethylammonium surfactant-immobilized cation exchange membranes for solid-phase extraction of phenolic compounds, Microchem. J., 96 (2010) 290–295.
[15] R.M. Marcé, F. Borrull, Solid-phase extraction of polycyclic aromatic compounds, J. Chromatogr., A, 885 (2000) 273–290.
[16] S. Ozgen, K. Sarıoglu, Synthesis and characterization of acrylonitrile-*co*-divinylbenzene (AN/DVB) polymeric resins for the isolation of aroma compounds and anthocyanins from strawberry, Food Bioprocess Technol., 6 (2013) 2884–2894.
[17] S. Zhu, W. Niu, H. Li, S. Han, G. Xu, Single-walled carbon nanohorn as new solid-phase extraction adsorbent for determination of 4-nitrophenol in water sample, Talanta, 79 (2009) 1441–1445.
[18] A.H. El-Sheikh, A.M. Alzawahreh, J.A. Sweileh, Preparation of an efficient sorbent by washing then pyrolysis of olive wood for simultaneous solid phase extraction of chloro-phenols and nitro-phenols from water, Talanta, 85 (2011) 1034–1042.
[19] E.I. Unuabonah, A. Taubert, Clay–polymer nanocomposites (CPNs): adsorbents of the future for water treatment, Appl. Clay Sci., 99 (2014) 83–92.
[20] S. Suresh, V.C. Srivastava, I.M. Mishra, Studies of adsorption kinetics and regeneration of aniline, phenol, 4-chlorophenol and 4-nitrophenol by activated carbon, Chem. Ind. Chem. Eng. Q., 19 (2013) 195–212.
[21] S.-H. Lin, R.-S. Juang, Adsorption of phenol and its derivatives from water using synthetic resins and low-cost natural adsorbents: a review, J. Environ. Manage., 90 (2009) 1336–1349.
[22] M. Ahmaruzzaman, Adsorption of phenolic compounds on low-cost adsorbents: a review, Adv. Colloid Interface Sci., 143 (2008) 48–67.
[23] P. Kubica, H. Garraud, J. Szpunar, R. Lobinski, Sensitive simultaneous determination of 19 fluorobenzoic acids in saline waters by solid-phase extraction and liquid chromatography–tandem mass spectrometry, J. Chromatogr., A, 1417 (2015) 30–40.
[24] J. Liu, G. Liu, W. Liu, Preparation of water-soluble β-cyclodextrin/poly(acrylic acid)/graphene oxide nanocomposites as new adsorbents to remove cationic dyes from aqueous solutions, Chem. Eng. J., 257 (2014) 299–308.
[25] W. Liu, X. Jiang, X. Chen, A novel method of synthesizing cyclodextrin grafted multiwall carbon nanotubes/iron oxides and its adsorption of organic pollutant, Appl. Surf. Sci., 320 (2014) 764–771.
[26] A. Li, Q. Zhang, G. Zhang, J. Chen, Z. Fei, F. Liu, Adsorption of phenolic compounds from aqueous solutions by a water-compatible hypercrosslinked polymeric adsorbent, Chemosphere, 47 (2002) 981–989.
[27] B. Pan, Q. Zhang, B. Pan, W. Zhang, W. Du, H. Ren, Removal of aromatic sulfonates from aqueous media by animated polymeric sorbents: concentration-dependent selectivity and the application, Microporous Mesoporous Mater., 116 (2008) 63–69.
[28] B. Pan, B. Pan, W. Zhang, L. Lv, Q. Zhang, S. Zheng, Development of polymeric and polymer-based hybrid adsorbents for pollutants removal from waters, Chem. Eng. J., 151 (2009) 19–29.
[29] M. Khajeh, S. Laurent, K. Dastafkan, Nanoadsorbents: classification, preparation, and applications (with emphasis on aqueous media), Chem. Rev., 113 (2013) 7728–7768.
[30] U. Baig, R.A.K. Rao, A.A. Khan, M.M. Sanagi, M.A. Gondal, Removal of carcinogenic hexavalent chromium from aqueous solutions using newly synthesized and characterized polypyrrole–titanium(IV)phosphate nanocomposite, Chem. Eng. J., 280 (2015) 494–504.
[31] M.A. Salem, R.G. Elsharkawy, M.F. Hablas, Adsorption of brilliant green dye by polyaniline/silver nanocomposite: kinetic, equilibrium, and thermodynamic studies, Eur. Polym. J., 75 (2016) 577–590.
[32] G. Tian, W. Wang, B. Mu, Y. Kang, A. Wang, Ag(I)-triggered one-pot synthesis of Ag nanoparticles onto natural nanorods as a multifunctional nanocomposite for efficient catalysis and adsorption, J. Colloid Interface Sci., 473 (2016) 84–92.
[33] C. Zhao, J. Xue, F. Ran, S. Sun, Modification of polyethersulfone membranes – a review of methods, Prog. Mater. Sci., 58 (2013) 76–150.
[34] N. Azum, K.A. Alamry, S.B. Khan, M. Abdul Rub, A.M. Asiri, Y. Anwar, Synergistic interaction between anionic and nonionic surfactant: application of the mixed micelles templates for the synthesis of silver nanoparticles, Int. J. Electrochem. Sci., 11 (2016) 1852–1867.
[35] N. Azum, S.B. Khan, M. Abdul Rub, A.M. Asiri, K.A. Alamry, Kinetic behavior of cobalt nanoparticles facilitated by cationic surfactant, Chem. Eng. Commun., 203 (2016) 446–451.
[36] L. Gzara, Z.A. Rehan, S.B. Khan, K.A. Alamry, M.H. Albeirutty, M.S. El-Shahawi, M.I. Rashid, A. Figoli, E. Drioli, A.M Asiri, Preparation and characterization of PES-cobalt nanocomposite membranes with enhanced anti-fouling properties and performances, J. Taiwan Inst. Chem. Eng., 65 (2016) 405–419.
[37] Z.A. Rehan, L. Gzara, S.B. Khan, K.A. Alamry, M.S. El-Shahawi, M.H. Albeirutty, A. Figoli, E. Drioli, A.M. Asiri, Synthesis and

characterization of silver nanoparticles-filled polyethersulfone membranes for antibacterial and anti-biofouling application, Recent Pat. Nanotechnol., 10 (2016) 231–251.
[38] S.B. Khan, K.A. Alamry, E.N. Bifari, A.M. Asiri, M. Yasir, L. Gzara, R.Z. Ahmad, Assessment of antibacterial cellulose nanocomposites for water permeability and salt rejection, J. Ind. Eng. Chem., 24 (2015) 266–275.
[39] K.-H. Nam, K. Seo, J. Seo, S.B. Khan, H. Han, Ultraviolet-curable polyurethane acrylate nanocomposite coatings based on surface-modified calcium carbonate, Prog. Org. Coat., 85 (2015) 22–30.
[40] M. Lim, H. Kwon, D. Kim, J. Seo, H. Han, S.B. Khan, Highly-enhanced water resistant and oxygen barrier properties of cross-linked poly(vinyl alcohol) hybrid films for packaging applications, Prog. Org. Coat., 85 (2015) 68–75.
[41] M. Lim, D. Kim, H. Han, S.B. Khan, J. Seo, Water sorption and water-resistance properties of poly(vinyl alcohol)/clay nanocomposite films: effects of chemical structure and morphology, Polym. Compos., 36 (2015) 660–667.
[42] H.M. Marwani, M.U. Lodhi, S.B. Khan, A.M. Asiri, Cellulose-lanthanum hydroxide nanocomposite as a selective marker for detection of toxic copper, Nanoscale Res. Lett., 9 (2014) 466–478.
[43] E.S. Jang, S.B. Khan, J. Seo, K. Akhtar, J. Choi, K.I. Kim, H. Han, Synthesis and characterization of novel UV-curable PU-Si hybrids: influence of silica on thermal, mechanical, and water sorption properties of polyurethane acrylates, Macromol. Res., 19 (2011) 1006–1013.
[44] I. Ahmad, T. Kamal, S.B. Khan, A.M. Asiri, An efficient and easily retrievable dip catalyst based on silver nanoparticles/chitosan-coated cellulose filter paper, Cellulose, 23 (2016) 3577–3588.
[45] D.-M. Han, G.-Z. Fang, X.-P. Yan, Preparation and evaluation of a molecularly imprinted sol–gel material for on-line solid-phase extraction coupled with high performance liquid chromatography for the determination of trace pentachlorophenol in water samples, J. Chromatogr., A, 1100 (2005) 131–136.
[46] B.H. Hameed, A.A. Rahman, Removal of phenol from aqueous solutions by adsorption onto activated carbon prepared from biomass material, J. Hazard. Mater., 160 (2008) 576–581.
[47] B.L. Woods, R.A. Walker, pH effects on molecular adsorption and solvation of *p*-nitrophenol at silica/aqueous interfaces, J. Phys. Chem. A, 117 (2013) 6224–6233.
[48] X.-Y. Gao, R.-L. Liu, J. Ma, H.-Y. Zhan, Z.-Q. Zhang, Combined dual-metal templates for fabrication of magnetic hierarchical porous carbon for highly efficient removal of 4-nitrophenol, J. Porous Mater., 23 (2016) 157–164.
[49] B. Zhang, F. Li, T. Wu, D. Sun, Y. Li, Adsorption of p-nitrophenol from aqueous solutions using nanographite oxide, Colloids Surf., A, 464 (2015) 78–88.
[50] A.E. Ofomaja, E.I. Unuabonah, Adsorption kinetics of 4-nitrophenol onto a cellulosic material, mansonia wood sawdust and multistage batch adsorption process optimization, Carbohydr. Polym., 83 (2011) 1192–1200.
[51] I. Langmuir, The constitution and fundamental properties of solids and liquids, J. Am. Chem. Soc., 38 (1916) 2221–2295.
[52] G. Mckay, H.S. Blair, J.R. Gardner, Adsorption of dyes on chitin. I. Equilibrium studies, J. Appl. Polym. Sci., 27 (1982) 3043–3057.
[53] H. Freundlich, Over the adsorption in solution, J. Phys. Chem., 57 (1906) 385–471.
[54] M.M. Rao, D.H.K.K. Reddy, P. Venkateswarlu, K. Seshaiah, Removal of mercury from aqueous solutions using activated carbon prepared from agricultural by-product/waste, J. Environ. Manage., 90 (2009) 634–643.
[55] R.-L. Tseng, P.-H. Wu, F.-C. Wu, R.-S. Juang, A convenient method to determine kinetic parameters of adsorption processes by nonlinear regression of pseudo-*n*th-order equation, Chem. Eng. J., 237 (2014) 153–161.